THEORY OF MARINE COMMUNITIES: COMPETITION, PREDATION, AND RECRUITMENT-DEPENDENT INTERACTION STRENGTH

SEAN R. CONNOLLY[1] AND JOAN ROUGHGARDEN

Department of Biological Sciences, Stanford University, Stanford, California 94305-5020 USA

Abstract. Of the marine animals that spend their adult lives inhabiting benthic communities, most have a planktonic larval phase. In this paper, we derive the relationship between the physical oceanographic processes that transport these larvae and the strength of species interactions in the benthic habitat. We review a model of hierarchical competition for space between two species with planktonic larvae and develop a model for predator–prey dynamics in which prey are space-limited. Lotka-Volterra approximations to these models are developed. The approximations provide per capita interaction strength (the effect of an individual of one species on the per capita growth rate of another) and population interaction strength (the effect of a population of one species on the per capita growth rate of another) as functions of parameters in the original model. Per capita and population interaction strengths of dominant competitors on subordinates decrease in magnitude as offshore advection of larvae increases. The per capita effect of prey on predators also decreases as offshore advection increases, but population interaction strength is independent of offshore advection rate. Conversely, the per capita effect of predators on prey is independent of offshore larval advection rate, but the population effect decreases as offshore advection increases. We also develop submodels that simulate experimental removals of competitors and predators. Measurements of interaction strength derived from these simulations decrease as offshore advection of larvae increases. These results predict that a latitudinal gradient in upwelling intensity in the northeast Pacific produces a gradient in the intensity of species interactions in rocky intertidal communities.

Key words: benthic/oceanic coupling; competition model; interaction strength; intertidal community; Lotka-Volterra model; oceanographic processes; planktonic larvae; predator–prey model; recruitment; upwelling.

INTRODUCTION

Ever since the classic papers of Connell (1961), Paine (1966), and Dayton (1971), the rocky intertidal zone has been a model system for the experimental study of ecological communities. Much of this work has consisted of species removal experiments. In these studies, the ecological role of a species is inferred by comparing control plots to plots from which the species has been experimentally added or excluded. One lesson that can be learned from this experimental work is that the local impact of particular species on communities varies a great deal depending on the timing, microhabitat, and geographical location of the study being conducted (see reviews in Underwood and Denley 1984, Menge and Farrell 1989, Menge 1991, Menge et al. 1994, Paine 1994).

Many of the animals that inhabit these communities have pelagic (oceangoing) larvae. Spatially and temporally variable recruitment of these species has emerged as an important cause of the variability in community dynamics found in experiments (e.g., Un-

derwood et al. 1983, Underwood and Denley 1984, Connell 1985, Roughgarden 1986, Fairweather 1988, Menge 1991, Menge et al. 1994, Booth and Brosnan 1995, Robles 1997). As a result, models of benthic communities have been modified to account for the effect of recruitment variation on the intensity and importance of species interactions (e.g., Menge and Sutherland 1987, Gaines and Lafferty 1995). In most of these models, larval supply is assumed to be independent of benthic community dynamics. When explaining differences among nearby local communities, such as exposed and protected habitats, this assumption is probably appropriate. Larvae can spend weeks to months in the plankton, allowing for considerable alongshore mixing. Recruits to nearby sites are drawn from a common larval pool, so differences in rates of larval supply to nearby communities are not likely to be affected by between-site differences in larval production rates.

At the regional scale, however, the sizes of larval populations are determined in part by adult stock sizes. Stock sizes, in turn, are affected by benthic interactions, such as competition and predation. To explain community structure patterns at this scale, we need to take into account two-way coupling between planktonic and benthic communities. For example, Gaines and

Lafferty (1995) modeled two-species competition for space in a local, open community. In their model, larvae of both species are continually supplied to the adult community from an external source. As a result, both species always coexist. In contrast, Iwasa and Roughgarden (1986) modeled a regional competition community in which larvae are produced by adults in local communities. Competition for space occurs exactly as in Gaines and Lafferty's model, but the species do not always coexist. Rather, each species must have a higher larval production to larval mortality ratio than the other, in at least one subpopulation. Thus, community structure at the regional scale may not be well characterized by models for open communities.

From this regional perspective, benthic community structure is affected by pelagic environmental conditions, because these conditions determine the probability that larvae will successfully recruit to the adult habitat. In particular, physical oceanographic processes may transport larvae great distances. Some of these processes carry larvae away from shore, inhibiting recruitment (Roughgarden et al. 1988, Gaines and Bertness 1992). Others transport larvae onshore, facilitating recruitment (Shanks 1983, Farrell et al. 1991, Piñeda 1991). Can these transport processes influence benthic species interactions? If so, how? To answer questions like these, we need to unite larval dynamics and benthic species interactions in a common theoretical framework.

A CASE STUDY: THE NORTHEAST PACIFIC

The North American Pacific coast is one of the most extensively studied marine environments in the world, both oceanographically and ecologically. This makes it an excellent region for which to construct a framework linking oceanographic processes to benthic community dynamics. We focus on the California Current System, which extends from southern Canada to Baja California, Mexico (U.S. GLOBEC 1994, Mann and Lazier 1996). Cross-shelf circulation in this region, particularly in the spring and summer, is dominated by upwelling. Upwelling occurs when strong equatorward winds, in conjunction with the coriolis effect, cause a surface layer of water to move offshore. Nearshore, this water is replaced by cold, saline, nutrient-rich water that emerges from depth (Pond and Pickard 1995).

Meroplanktonic larvae become entrained in these offshore-moving surface currents and accumulate at fronts where this upwelled water meets the offshore, southward-flowing water of the California Current (Roughgarden et al. 1988, 1994, Wing et al. 1995, Grantham 1997). These larvae must return to the coast in order to recruit to adult populations. This occurs primarily during relaxation events, when upwelling-favorable winds weaken and the front moves onshore (Roughgarden et al. 1988, 1991, Farrell et al. 1991, Wing et al. 1995). Spatial variation in recruitment also depends on upwelling intensity. Higher recruitment tends to occur where offshore transport is weaker and fronts are more nearshore (Ebert and Russell 1988, Miller 1992, Wing et al. 1995, Grantham 1997).

Intertidal communities in the northern part of this region have been studied for decades. Clear geographical trends emerge from this work. On the outer coasts of Washington and Oregon, species removal experiments indicate that the allocation of space among mussels and barnacles is determined primarily by species interactions, particularly competition and predation (Paine 1966, 1974, Farrell 1989, 1991, Menge et al. 1994). In contrast, studies in central and northern California indicate that rates of larval supply largely determine adult abundances, whereas species interactions have smaller effects (Gaines and Roughgarden 1985, Wing et al. 1995, Grantham 1997; T. M. Farrell, *unpublished data*, J. S. Pearse, *unpublished data*).

These geographical differences in community structure correspond to marked differences in upwelling intensity. Upwelling off the coasts of Oregon and Washington is weak: the upwelling season is short, the offshore advection rate is low, fronts are nearshore, and relaxation events are frequent. In contrast, upwelling off central and northern California is strong: the upwelling season is long, the offshore advection rate is high, fronts are far from shore, and relaxation events are infrequent (Parrish et al. 1981, Huyer 1983, U.S. GLOBEC 1994). This association between oceanographic regime and community structure inspired the hypothesis that higher larval supply in Oregon and Washington, promoted by weaker upwelling, is responsible for the community structure differences (Roughgarden et al. 1988). High larval supply makes free space scarce, so competitive and predator–prey interactions regulating access to that space should be more important in Oregon and Washington than in central and northern California.

OBJECTIVES

Our goal in this study is to characterize the link between larval transport processes and the strength of species interactions in the benthic habitat. In particular, we wish to determine whether there are theoretical grounds to support the hypothesis that there is a latitudinal gradient in interaction strength in the northeast Pacific rocky intertidal, and that it is caused by a latitudinal gradient in upwelling intensity (Roughgarden et al. 1988). Toward that end, we review a previously proposed model coupling hierarchical competition for space with oceanic larval transport (Connolly and Roughgarden 1998), and we develop a model coupling predation on space-limited prey with oceanic larval transport. These models can be used to determine the effects of changes in upwelling intensity on competitive and predator–prey interaction strengths. We investigate three definitions of interaction strength:

1) *Per capita interaction strength.* We define per capita interaction strength as the effect of an individual

of one species on the per capita population growth rate of a competitor, prey, or predator.

2) *Population interaction strength.* We define population interaction strength as the net effect of a population of one species on the per capita population growth rate of another (cf. Navarrete and Menge 1996). As upwelling intensity changes, species abundances, as well as per capita interaction strengths, may change. Population interaction strength captures the combined effects of changes in abundance and changes in per capita interaction strength.

3) *Local interaction strength.* We define local interaction strength as the effect of a species' removal from a local, open community (such as an experimental plot) on the abundances of the remaining species (e.g., Paine 1980).

To determine per capita and population interaction strengths, Lotka-Volterra approximations to the models are developed. The terms in these approximations are functions of parameters in the original model, including larval transport parameters. These models can be written in the form

$$\frac{dN_i(t)}{dt} = \left[r_i + \sum_j \lambda_{ij} N_j(t) \right] N_i(t) \qquad (1)$$

where r_i is the intrinsic rate of increase of species i, N_j is the abundance of species j, and λ_{ij} is the per capita interaction strength of species j on species i. The population interaction strength of species j on i, then, is simply

$$\Lambda_{ij} = \lambda_{ij} N_j. \qquad (2)$$

In this study, N_j is evaluated at the interior equilibrium, i.e., the equilibrium at which the species coexist.

To determine local interaction strengths, we develop submodels that simulate population dynamics in two types of plots: those from which competitors or predators have been excluded and those in which competitors or predators are present. Local interaction strength can be measured as the relative difference in abundances between these plots (Paine 1992):

$$I_{ij} = \frac{N_i^E - N_i^C}{N_i^C} \qquad (3)$$

where N_i^E is the density of species i in experimental plots, and N_i^C is density of species i in control plots. In this paper, experimental plots are considered to be those from which competitors or predators are excluded, and control plots are considered to be those in which species interactions are allowed to proceed normally. We derive the local interaction strength of competitive dominants on subordinates and of predators on prey. We do not derive the effect of prey on predators, because this would correspond to an experiment in which all prey were removed from experimental plots. Clearly, all predators in such plots would die before reaching adult size.

The hypothesis under investigation pertains specif-

ically to the larval transport processes associated with upwelling (Roughgarden et al. 1988). Therefore, in this paper, the term upwelling refers specifically to offshore advection rates and front positions, and not to other upwelling-mediated environmental changes that might also affect benthic communities (e.g., water temperature or phytoplankton productivity). This study is not a comprehensive investigation of the effects of upwelling on benthic communities. Rather, it is a targeted study of a particular possible causal link between upwelling and benthic community structure.

To limit the number of figures presented, gradients in offshore advection rate are shown, but corresponding gradients in front position are not. However, the qualitative relationships hold with respect to both parameters: where a quantity increases with offshore advection rate, it also increases as the front moves offshore, etc. Because increasing upwelling is associated with increasingly offshore fronts as well as stronger offshore advection, the magnitude of gradients shown in figures will tend to be conservative with respect to the overall effect of upwelling.

The Models

The models extend a previously developed one-dimensional, single-species model for barnacles, coupling benthic population dynamics with oceanic larval transport (Alexander and Roughgarden 1996). In that model, larvae are distributed between the coast and an offshore front. At the coast, larvae are spawned by adults and recruit to free space in the adult habitat. Analysis of the model confirmed that the increasing offshore advection and further offshore fronts associated with increasing upwelling produce lower recruitment and adult abundances. Simulations of time-varying advection and front position were used to explore the effects of relaxation events on population dynamics. This produced temporal fluctuations in recruitment and adult abundances, but the overall relationships among upwelling, recruitment, and adult abundance were the same: the less frequent relaxation events associated with strong upwelling led to lower mean recruitment and adult abundances (Alexander and Roughgarden 1996). In this paper, we focus on the constant advection, stationary front case. This makes analytical derivations of interaction strengths possible. As a result, the response of interaction strength to upwelling can be characterized by simply plotting a function against advection and front position, rather than by running a series of lengthy numerical simulations. This allows us to explore a much wider range of parameter values. However, because relaxation events are not incorporated, this study probably underestimates the sensitivity of community structure to changes in upwelling intensity (Alexander and Roughgarden 1996).

Competition model

Competition for space in the northeast Pacific rocky intertidal zone can be strongly hierarchical, particularly among mussels and barnacles. The strong shells, large size, and overgrowth ability of the California sea mussel, *Mytilus californianus*, enable it to outcompete barnacles, algae, and other mussels for primary space (Paine 1966, 1974). Among acorn barnacles, competitive dominants may settle on, overgrow, or undercut subordinates (Connell 1961, Farrell 1991). To determine the effect of upwelling on benthic competition, we analyze a model first formulated elsewhere (Connolly and Roughgarden 1998). The model approximates the interactions previously described by allowing the dominant to settle on, and replace, the subordinate (cf. Hastings 1980, Tilman 1994, Dial and Roughgarden 1998). In contrast, the subordinate can settle only on vacant space. Settlement is a mass-action process for both populations, an assumption that is probably more appropriate for acorn barnacles than for leaf barnacles or mussels (Seed 1976, Petersen 1984, Gaines and Roughgarden 1985, Satchell and Farrell 1993). Adult mortality occurs at a density-independent rate. This assumption may not hold when free space is scarce (Gaines and Roughgarden 1985), but the incorporation of density-dependent mortality does not appear to qualitatively change the results (see *Discussion*). With these assumptions, adult dynamics are

$$\frac{dN_1(t)}{dt} = c_1 L_1(0, t)[F(t) + a_2 N_2(t)] - \mu_1 N_1(t) \quad (4a)$$

$$\frac{dN_2(t)}{dt} = c_2 L_2(0, t)F(t) - \mu_2 N_2(t)$$
$$- c_1 L_1(0, t)a_2 N_2(t) \quad (4b)$$

where the subscript 1 denotes the dominant and 2 denotes the subordinate. $N_i(t)$ is the adult population size per unit length of coastline at time t, $L_i(0, t)$ is the abundance of larvae at the coast per unit surface area of the ocean at time t, $F(t)$ is benthic free space per unit length of coastline, c_i is the per capita rate at which larvae at the coast settle onto free space, a_i is the basal area of an adult, and μ_i is the adult mortality rate. Unoccupied space fluctuates according to

$$F(t) = A - a_1 N_1(t) - a_2 N_2(t) \quad (4c)$$

where A is total benthic habitat area per unit length of coastline. Larvae move between the coast and an offshore front by offshore transport (advection) and turbulent mixing (diffusion). Advection is proportional to larval abundance, and diffusion is proportional to the spatial gradient in larval abundance (Okubo 1980, Holmes et al. 1994, Alexander and Roughgarden 1996). The larval mortality rate is independent of density (Alexander and Roughgarden 1996, Strathmann 1996). Thus, larval dynamics in space and time are as follows:

$$\frac{\partial L_i(x, t)}{\partial t} = -u_i \frac{\partial L_i(x, t)}{\partial x} + k_i \frac{\partial^2 L_i(x, t)}{\partial x^2} - v_i L_i(x, t). \quad (5)$$

$L_i(x, t)$ is the larval abundance per unit surface area of ocean at offshore location x at time t, u_i is the offshore larval advection rate, k_i is the larval diffusion coefficient, and v_i is the larval mortality rate. Values of x range from 0 at the coast to x_f at the offshore front. The front is a reflecting boundary for both species:

$$u_i L_i(x_f, t) - k_i \frac{\partial L_i(x_f, t)}{\partial x}\bigg|_{x=x_f} = 0. \quad (6)$$

The flux of larvae through the coastal boundary is the difference between the rate at which larvae enter the larval population from the benthic habitat (larval production) and the rate at which they leave the larval population to enter the benthic habitat (settlement):

$$u_i L_i(0, t) - k_i \frac{\partial L_i(0, t)}{\partial x}\bigg|_{x=0}$$
$$= m_1 N_1(t) - c_1 L_1(0, t)[F(t) + a_2 N_2(t)] \quad (7a)$$

$$u_2 L_2(0, t) - k_2 \frac{\partial L_2(0, t)}{\partial x}\bigg|_{x=0}$$
$$= m_2 N_2(t) - c_2 L_2(0, t)F(t). \quad (7b)$$

Larvae are produced by adults at density-independent rate m_i, and leave the population by settling on available space in the adult habitat. Again, the subordinate can settle only on vacant space, whereas the dominant can also settle on space occupied by the subordinate.

Predator–prey model

The ochre seastar, *Pisaster ochraceus*, is the principal predator in the rocky intertidal communities of central California and the Pacific Northwest (Paine 1966, 1974, 1976, Gaines and Roughgarden 1985, Menge et al. 1994, Possingham et al. 1994, Navarrete and Menge 1996). Like barnacles, *P. ochraceus* has planktonic larvae (Strathmann 1987), so we assume that both predator and prey populations have a planktonic larval stage. Prey recruit only to free space, but predators recruit anywhere in the adult habitat. We have been unable to find studies that characterize the functional response of seastars. Therefore, we assume a linear functional response. This keeps the model simple and increases the comparability of the results with experimental estimates of interaction coefficients for intertidal predators, which also assume a linear functional response (Navarrete and Menge 1996). As in the competition model, adult mortality rates are density independent. With these assumptions, adult dynamics are

$$\frac{dN_1(t)}{dt} = c_1 L_1(0, t)F(t) - \mu_1 N_1(t) - e N_1(t)N_2(t) \quad (8a)$$

$$\frac{dN_2(t)}{dt} = c_2 A L_2(0, t) - \mu_2 N_2(t) \quad (8b)$$

where

TABLE 1. Physical and biological parameters used in figures.

Parameter	Description	Values
Physical parameters		
A	adult habitat area/100 m of coastline	$A = 100$ m^2
u	offshore advection rate	variable, 50–150 m/h
k	eddy-diffusion coefficient	$k = 36000$ m^2/h
x_f	location of offshore front	$x_f = 30000$ m
Competition parameters		
a_i	basal area of an adult	$a_1 = 0.0001$ m^2
		$a_2 = 0.00005$ m^2
c_i	settlement coefficient	$c_1 = c_2 = 0.02$/h
μ_i	adult mortality rate	$\mu_1 = \mu_2 = 0.0002$/h
m_i	larval production rate	$m_1 = 0.024$/h
		$m_2 = 0.15$/h
ν_i	larval mortality rate	$\nu_1 = \nu_2 = 0.002$/h
Predator–prey parameters		
a_i	basal area of adult prey	$a_1 = 0.0001$ m^2
c_i	settlement coefficient	$c_1 = 0.02$/h
		$c_2 = 0.0001$/h
μ_i	adult mortality rate	$\mu_1 = 0.0005$/h
		$\mu_2 = 0.00001$/h
m_1	prey larval production rate	$m_1 = 0.05$/h
b_2	predator larvae produced/ prey consumed	$b_2 = 0.06$
ν_i	larval mortality rate	$\nu_1 = \nu_2 = 0.002$/h
e	encounter rate	$e = 0.00001$/h

$$F(t) = A - a_1 N_1(t). \tag{8c}$$

The subscript 1 denotes the prey and 2 denotes the predator. Otherwise, $N_i(t)$, $L_i(0, t)$, $F(t)$, c_i, A, a_i, and μ_i have the same meanings as in Eq. 4. The rate at which predators encounter and consume prey is designated e. Because population sizes are in units of abundance per unit length coastline, the encounter rate is the proportion of habitat area in one unit length of coastline (A) that is searched per unit time. For instance, $e = 0.1$ means that, in one unit of time, a predator searches 10% of the benthic habitat in a unit length of coastline. Larval population dynamics of both species follow Eq. 5, with frontal boundary conditions given by Eq. 6. Coastal boundary conditions are

$$u_1 L_1(0, t) - k_1 \frac{\partial L_1(0, t)}{\partial x}\bigg|_{x=0}$$

$$= m_1 N_1(t) - c_1 L_1(0, t)F(t) \tag{9a}$$

$$u_2 L_2(0, t) - k_2 \frac{\partial L_2(0, t)}{\partial x}\bigg|_{x=0}$$

$$= b_2 e N_1(t)N_2(t) - c_2 A L_2(0, t). \tag{9b}$$

Here, b_2 is the number of predator larvae produced per prey consumed. Other parameters and state variables have the same meanings as in Eq. 7.

Parameters

Parameter values used for the figures are presented in Table 1. We used oceanographic parameter values that are reasonable for the California Current System

(Okubo 1971, Alexander and Roughgarden 1996), and we assumed that the larvae of all species are subject to the same transport processes, i.e., $u_1 = u_2 = u$ and $k_1 = k_2 = k$. Where possible, biological parameters for the dominant competitor were based on field studies of the barnacle *Balanus glandula*, parameters for the subordinate were based on the barnacles *Chthamalus dalli* and *Chthamalus fissus*, and parameters for the predator were based on the seastar *Pisaster ochraceus*. Parameter values for the prey were intermediate between *Balanus* and *Chthamalus*.

Because a purely analytical study of the responses of interaction strengths to upwelling was not possible, we explored a range of values around our parameter estimates to insure that the results reported in this paper are not sensitive to the choice of a particular parameter set. We varied each parameter individually, holding the others at the baseline values reported in Table 1. We identified the largest and smallest parameter values within this range for which the interacting populations coexisted across the range of advection rates considered (50–150 m/h), and we verified that the results did not change qualitatively with these parameter values. Where we report that a quantity increases with, decreases with, or is insensitive to upwelling intensity, that relationship holds for all parameter sets considered. Similarly, the accuracy of the approximations illustrated in the figures is characteristic of all parameter sets that we explored.

To our knowledge, field estimates of larval mortality rates have not been made for these species. The only published estimates of barnacle larval mortality are for northern Atlantic species (Pyefinch 1948), an estimate (5% per day or 0.002/h) that has been used previously to model barnacle population dynamics (Possingham and Roughgarden 1990, Alexander and Roughgarden 1996). We know of no such field estimates for seastars. Therefore, we used 5% per day as a baseline for all species and considered a range of larval mortality rates from 1% to 10% per day (0.0005/h to 0.004/h).

The settlement coefficient of *Balanus* has been calculated from simultaneous field measurements of larval concentrations, benthic free space, and settlement rates (Gaines et al. 1985, Possingham and Roughgarden 1990). To our knowledge, no field measurements of settlement coefficients have been made for *Chthamalus* or *Pisaster*. Therefore, we used the settlement coefficient of *Balanus* (0.02/h) as a baseline for the dominant competitor, subordinate competitor, and prey, and we considered variation of an order of magnitude in either direction of this value. *Pisaster* larvae take 76–228 d to metamorphose in the laboratory (Strathmann 1978), whereas *Balanus* and *Chthamalus* take ~15–20 days (Brown and Roughgarden 1985, Miller et al. 1989). This means that the fraction of the *Pisaster* larval population that is competent to settle, assuming 5% mortality per day, will be anywhere from 1/10 to 1/10 000 as large as the fraction of the barnacle larval population

that is competent. Therefore, we considered a wide range of predator settlement coefficients based on these fractions (0.002/h to 0.000002/h). We used an intermediate value (0.0001/h) for the figures presented in this paper.

Gaines and Roughgarden (1985) found that mortality rates for adult *Balanus* from sources other than seastar predation are <20% per week, and average ~5% per week, independent of age. Similarly, adult mortality rates estimated from life tables for *Chthamalus fissus* are ~5% per week (Hines 1976). Therefore, we considered a range of mortality rates from 2% to 20% per week (0.0001/h to 0.001/h) for the prey, dominant competitor, and subordinate competitor populations. Field data on *Pisaster ochraceus* (Menge 1975) indicate an annual adult mortality rate of only 5%, or ~0.00001/h (Ebert 1996). We took this as a baseline and considered mortality rates from 1% to nearly 90% per year.

Possingham and Roughgarden (1990) describe a procedure for calculating average larval production rate, and estimate this from field data on *Balanus glandula* (Hines 1976). We used this estimate (0.024/h) for our dominant competitor, and we used the same procedure to estimate larval production rates for the subordinate (0.15/h) from the same study (Hines 1976). To determine whether differences in larval production rates between populations affected our results, we considered a range of larval production rates (0.01/h to 1/h) for both species.

An age-averaged estimate of predator larval production per prey consumed, b_2, requires (1) the fraction of the predator population that is reproductively mature, (2) the average energy content of prey, (3) the proportion of that energy that a mature seastar converts into eggs, (4) the energy content of eggs, (5) fertilization success, and (6) survivorship from zygote to larval stage. We estimated these components as follows:

1) Assuming 95% annual survival (Ebert 1996) and reproductive maturity at 5 yr (Menge 1975), ~75% of the postsettlement predator population is mature.

2) We assume that prey tissue contains 18.8 kJ/g dry mass, a reasonable value for barnacles (Harrold 1981). At a mortality rate of 0.0005/h (Gaines and Roughgarden 1985), the average prey is ~2 mo old. Because neither *Chthamalus* nor *Balanus* matures before this age, upper bounds for age-averaged body mass can be taken as the smallest body mass for which brood masses are reported (~0.1 mg for *Chthamalus* and 0.8 mg for *Balanus*), yielding energy contents of ~1.67 J and 14.65 J, respectively. We used an intermediate value, 4.19 J (one calorie), for our estimate of a baseline value for b_2.

3) *Pisaster giganteus* in central California allocates ~10% of its annual energy intake to reproduction (Harrold 1981). However, the majority of species on which *P. giganteus* preys provide much more energy per time spent feeding than do barnacles (Harrold 1981). Be-

cause seastars may allocate less energy to reproduction as their energy intake declines (Nimitz 1971, Harrold 1981), we used a smaller value, 5%, for our estimate of b_2.

4) The energy content of predator eggs can be estimated by multiplying their volume, $2 \times 10^6 \ \mu m^3$ for *P. ochraceus* (Strathmann and Vedder 1978), by their organic density, for which 400 $\mu g/mm^3$ is a reasonable value for echinoderms (Turner and Lawrence 1979). Assuming that the allocation of this organic matter to protein, lipid, and carbohydrate is 60%, 35%, and 5%, respectively (Turner and Lawrence 1979), the energy content of a predator egg is ~0.02 J.

5) Estimates of fertilization success in free-spawning marine invertebrates vary from nearly 100% to as low as 0.01% (Denny and Shibata 1989, Sewell and Levitan 1992). We used an intermediate value of 1%.

6) We have found no measurements of postfertilization mortality in the field, so we assume that this rate is comparable to that of larval mortality, 5% per day. If it takes 5 d for zygotes to develop into larvae (Strathmann 1987), then ~75% of zygotes become larvae.

From these values, we obtain 0.06 predator larvae produced per prey consumed. Because of the uncertainties involved in estimating several of the described quantities, we considered a range of values from 0.0001 to 1 larva per prey.

Although we have been unable to find measurements of the rates at which *Pisaster ochraceus* locates and consumes intertidal barnacles, we can base an estimate on studies of other species. *Pisaster giganteus* consumes acorn barnacles (mostly *Balanus aquila, B. nubilus,* and *B. crenatus*) at a rate of about 5 barnacles/d (Harrold 1981). Adult sizes of these barnacles range from ~10 to 130 mm diameter (Newman and Abott 1980). If we assume that the average prey basal area is 0.002 m² (i.e., 50 mm diameter), then this yields an encounter rate of 0.000002 m²/h or $e = 0.00000002/h$. This rate corresponds to the extreme case in which there is 100% cover, and the predator is eating continuously as it moves through the habitat. Because seastars may move faster through habitat in which prey are less abundant, we treated this value as a lower bound on the encounter rate and considered values up to six orders of magnitude higher, 2 m²/h or $e = 0.02/h$. We used an intermediate value, $e = 0.00001/h$, for the figures presented in this paper (Table 1).

RESULTS

Competition model

Scaling argument.—The benthic dynamics can be characterized with a two-equation scaling approximation (Alexander and Roughgarden 1996, Connolly and Roughgarden 1998). This approximation takes advantage of the fact that larval dynamics occur on a faster time scale (days to weeks) than the growth and mat-

uration of newly settled larvae (months). Because newly settled larvae are very small, they occupy a negligible amount of space in the benthic habitat and do not reproduce. Therefore, over the time scale at which larval populations equilibrate, free space and larval production by adults are relatively constant. These observations allow us to provisionally treat adult population sizes as constants and to solve Eqs. 5–7 for the larval equilibria at the coast:

$$\hat{L}_1(0, N_1) = \frac{2m_1 N_1 q_1}{2c_1 q_1(A - a_1 N_1) + 1} \quad (11a)$$

$$\hat{L}_2(0, N_1, N_2) = \frac{2m_2 N_2 q_2}{2c_2 q_2(A - a_1 N_1 - a_2 N_2) + 1} \quad (11b)$$

where q_1 and q_2 are the species-specific water column properties

$$q_i = [e^{1/2[u_i - \sqrt{4k_i v_i + u_i^2}]x_i/k_i}(u_i + \sqrt{4k_i v_i + u_i^2})$$
$$- e^{1/2[u_i + \sqrt{4k_i v_i + u_i^2}]x_i/k_i}(u_i - \sqrt{4k_i v_i + u_i^2})]$$
$$\times [(2u_i^2 - 4k_i v_i)$$
$$\times (e^{1/2[u_i - \sqrt{4k_i v_i + u_i^2}]x_i/k_i} - e^{1/2[u_i + \sqrt{4k_i v_i + u_i^2}]x_i/k_i})]^{-1}.$$
$$(12)$$

Here, q_i represents the combined effects of larval mortality, offshore advection, and turbulent mixing on the abundance of larvae at the coast. Substituting Eq. 11 for $L_1(0, t)$ and $L_2(0, t)$ in Eq. 4, adult dynamics become

$$\frac{dN_1}{dt} = c_1\hat{L}_1(0, N_1)(A - a_1 N_1) - \mu_1 N_1 \quad (13a)$$

$$\frac{dN_2}{dt} = c_2\hat{L}_2(0, N_1, N_2)(A - a_1 N_1 - a_2 N_2)$$
$$- \mu_2 N_2 - c_1\hat{L}_1(0, N_1)a_2 N_2. \quad (13b)$$

Although this approximation has been justified verbally and used previously (Alexander and Roughgarden 1996, Connolly and Roughgarden 1998), its quantitative accuracy has never been verified. To do this, we numerically analyzed the approximation (Eq. 13) and the full model (Eqs. 4–7), and we compared their dynamics (see Hirsch 1988 for an introduction to numerical analysis). The two models agree extremely closely (Fig. 1), so we use the scaling approximation in lieu of the full model in all subsequent analyses. Hereafter, we refer to the scaling approximation as the "original model" to avoid confusion with the Lotka-Volterra approximation.

Lotka-Volterra approximation.—Because the model is now in the form of coupled ordinary differential equations, the benthic dynamics can be approximated with Lotka-Volterra competition equations (Eq. 1). This approximation, detailed in Appendix A, yields the following:
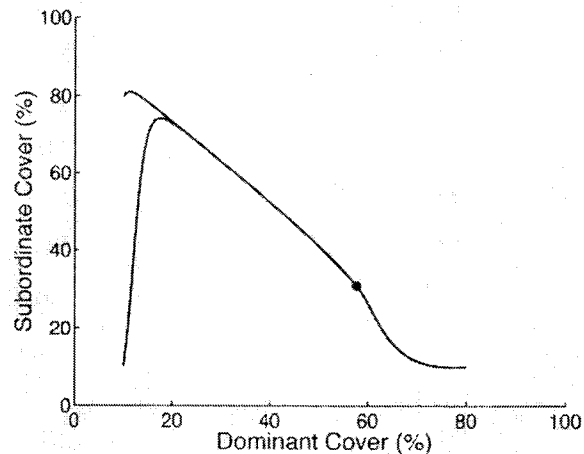

FIG. 1. Comparison of the scaling approximation and the full competition model. The solid lines are trajectories to equilibrium of the full model from three different initial conditions. Trajectories of the scaling approximation from the same three initial conditions are plotted with dashed lines. Dashed lines are not separately visible alongside solid lines, because the solid lines and dashed lines overlap, i.e., the trajectories of the full model and scaling approximation coincide so closely that they are not visually distinguishable. The equilibrium is marked with a solid circle. Trajectories were determined using numerical analysis. Benthic dynamics for both models were predicted with a forward-time scheme. Larval dynamics for the full model were predicted with a control volume, forward-time, centered-space scheme (Patankar 1980, Hirsch 1988). The simulations were run using MATLAB (1994). The scripts are available as a supplemental file in *Ecological Archives*. The offshore advection rate, u, is 100 m/h.

$$r_1 = \frac{(m_1 - \mu_1)p_1}{m_1} \quad (14a)$$

$$r_2 = \frac{(m_2 - \mu_2)p_2}{m_2}$$
$$+ \frac{p_1 a_2[p_1 a_2 m_1(2Ac_2 q_2 + 1) + a_1(p_1 m_2 - 2m_1 p_2)]}{m_1 m_2 a_1^2}$$
$$(14b)$$

$$\lambda_{11} = -\frac{2c_1 q_1 a_1(m_1 - \mu_1)^2}{m_1} \quad (14c)$$

$$\lambda_{22} = -\frac{2a_2 c_2 q_2[a_1(m_2 - \mu_2) - a_2 p_1]^2}{m_2 a_1^2} \quad (14d)$$

$$\lambda_{12} = 0 \quad (14e)$$

$$\lambda_{21} = -\left(\frac{2c_2 q_2[a_2 p_1 - a_1(m_2 - \mu_2)]^2}{a_1 m_2}\right.$$
$$\left. + \frac{2c_1 q_1 a_2(m_1 - \mu_1)^2(2Ac_1 q_1 + 1)}{m_1}\right) \quad (14f)$$

where p_i is the single-species positivity requirement from the scaling approximation,

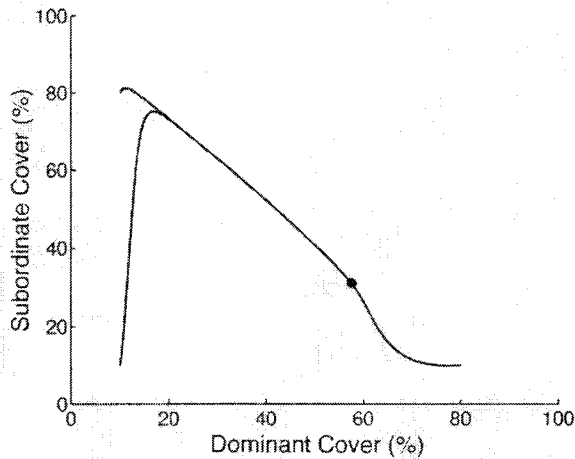$$p_i = -\mu_i + 2Ac_i(m_i - \mu_i)q_i \quad (15)$$

FIG. 2. Comparison of the Lotka-Volterra approximation and the scaling approximation for the competition model. Trajectories were determined with the MATLAB (1994) function ode45, which uses fourth- and fifth-order Runge-Kutta formulas. The solid lines are trajectories to equilibrium of the scaling approximation from three different initial conditions. Trajectories of the Lotka-Volterra approximation from the same three initial conditions are plotted with dashed lines. Dashed lines are not separately visible alongside solid lines, because the trajectories of the two models coincide. The equilibrium is marked with a solid circle. The offshore advection rate, u, is 100 m/h. Note the remarkable similarity between these trajectories and those plotted in Fig. 1.

(Alexander and Roughgarden 1996). If $p \leq 0$, the population cannot persist, even in the absence of its competitor.

Numerical analysis demonstrates that the Lotka-Volterra approximation agrees closely with the original model, even far from the interior equilibrium (Fig. 2). The approximation is accurate throughout the parameter space that we explored because the terms in the approximation are functions of parameters in the original model. Thus, the terms in Eq. 14 change as the parameters of the original model change.

Lotka-Volterra competition equations are often written in a form that includes terms for carrying capacities and competition coefficients rather than per capita interaction strengths. These terms can be obtained from Eq. 14. Carrying capacity is a population's equilibrium abundance in the absence of its competitor,

$$K_i = \frac{r_i}{\lambda_{ii}} \tag{16}$$

and the competition coefficient is the intensity of interspecific competition relative to the intensity of intraspecific competition,

$$\alpha_{ij} = \frac{\lambda_{ij}}{\lambda_{ii}} \tag{17}$$

Fig. 3 plots intrinsic growth rates, carrying capacities, and competition coefficients as functions of offshore advection. Intrinsic growth rates and carrying capacities decrease as upwelling increases. Competi-

tion coefficients are comparatively insensitive to upwelling, although α_{21} actually declines slightly in Fig. 3C.

Adult abundances.—Adult abundances equilibrate at

$$\hat{N}_1 = \frac{r_1}{\lambda_{11}} \tag{18a}$$

$$\hat{N}_2 = -\frac{1}{\lambda_{22}}\left(r_2 - \frac{\lambda_{21}}{\lambda_{11}}r_1\right). \tag{18b}$$

As we have noted elsewhere, percent cover of the dominant decreases as upwelling intensity increases, but percent cover of the subordinate actually increases with upwelling intensity (Connolly and Roughgarden 1998). This is illustrated in Fig. 4.

Interaction strengths.—The per capita strengths of interspecific competition can be obtained directly from the Lotka-Volterra approximation according to Eq. 1. Obviously, because there is no effect of the subordinate on the dominant (Eq. 14e), λ_{12} is independent of upwelling intensity. However, the per capita interaction strength of the dominant on the subordinate (Eq. 14f) decreases in magnitude as upwelling increases (Fig. 5A).

Population interaction strengths (Eq. 2), evaluated at the interior equilibrium, are

$$A_{12} = 0 \tag{19a}$$

$$A_{21} = -\frac{\lambda_{21}}{\lambda_{11}}r_1. \tag{19b}$$

Like the per capita interaction strengths, there is no effect of the subordinate on the dominant, but the population interaction strength of the dominant on the subordinate decreases in magnitude as upwelling increases (Fig. 5B).

Local interaction strengths (Eq. 3) can be obtained by simulating small-scale species removal experiments. We can explore the effect of upwelling on these experiments by recognizing that small experimental and control plots are essentially open systems for species with planktonic larvae. Larval supply to these plots is determined at the regional scale, and is a function of larval transport processes (Eq. 11). Appendix B describes a submodel that simulates experimental removals of competitive dominants. The submodel includes small experimental and control plots nested within a regional system. In the experimental plot, dominants are removed and prevented from colonizing. In the control plot, dominants are present and are allowed to recruit normally. From subordinate abundances in these two plots, local interaction strength can be calculated according to Eq. 3. We can then determine how this quantity varies with characteristics of the regional system, such as upwelling intensity. At equilibrium, local interaction strength is evaluated as follows:
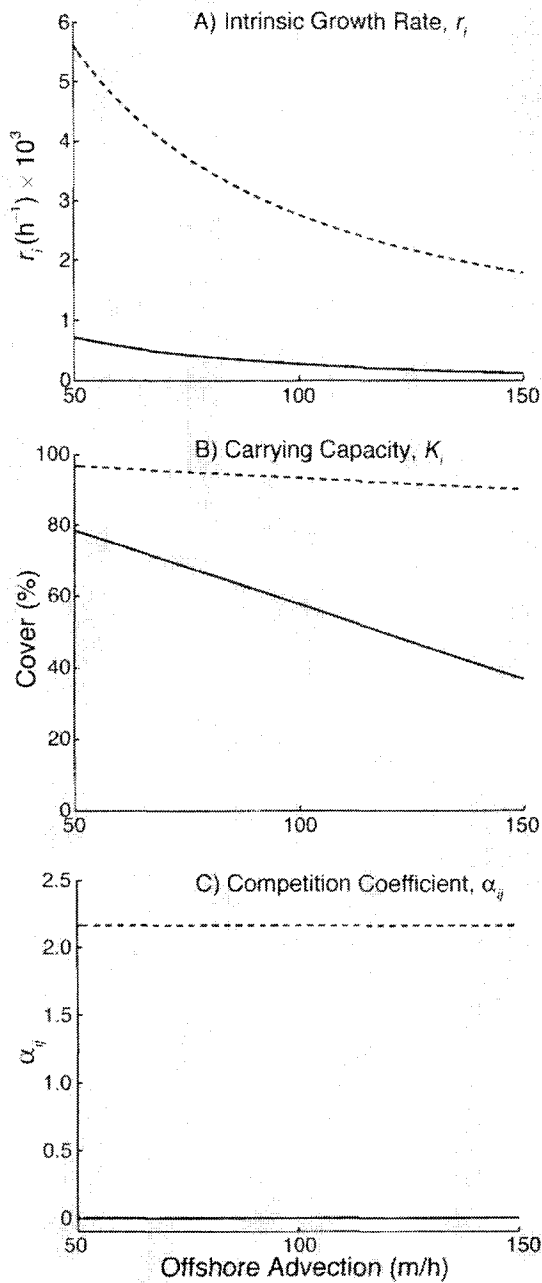
moval of the dominant and (2) the subordinate's ability to colonize that additional space (its recruitment rate). Fig. 5C illustrates that local interaction strength decreases as upwelling increases. In practice, experimentalists often cannot determine when or whether abundances in their plots have reached equilibrium. Therefore, we ran numerical simulations to verify that this trend holds when interaction strength is measured before the plots reach equilibrium. In the simulations, experiments were initiated at the same time in systems with differences in upwelling intensity, and interaction strength was plotted as a function of time until all plots equilibrated. The simulations confirm that interaction strengths are lower in regions of stronger upwelling, even when interaction strength is measured before any or all of the plots have reached equilibrium (results are not shown).

Predator–prey model

Scaling argument.—Following the procedure outlined for the competition model, benthic predator–prey dynamics can be approximated with

$$\frac{dN_1}{dt} = c_1 \hat{L}_1(0, N_1)(A - a_1 N_1) - \mu_1 N_1 - e N_1 N_2 \quad (21a)$$

$$\frac{dN_2}{dt} = c_2 \hat{L}_2(0, N_1, N_2)A - \mu_2 N_2 \quad (21b)$$

where

$$\hat{L}_1(0, N_1) = \frac{2m_1 N_1 q_1}{2c_1 q_1 (A - a_1 N_1) + 1} \quad (22a)$$

$$\hat{L}_2(0, N_1, N_2) = \frac{2b_2 e N_1 N_2 q_2}{2Ac_2 q_2 + 1}. \quad (22b)$$

Here, q_1 and q_2 are the species-specific water column properties of Eq. 12. As in the competition model, nu-

FIG. 3. Sensitivity of Lotka-Volterra parameters (competition model) to offshore advection rate. In (A) and (B), the solid line represents the competitive dominant, and the dashed line represents the subordinate. In (C), the solid line represents α_{12}, and the dashed line represents α_{21}. The rates in panel (A) have been multiplied by a factor of 10^3.

$$I_{21} = \frac{2Ac_1 q_1 c_2 q_2 (m_1 - \mu_1)[a_2 p_1 - a_1(m_2 - \mu_2)]}{a_2 c_1 q_1 p_1 (m_1 - \mu_1) + c_2 q_2 \mu_1 [a_2 p_1 - a_1(m_2 - \mu_2)]}. \quad (20)$$

This represents the combined effect of (1) the additional space made available to the subordinate by re-
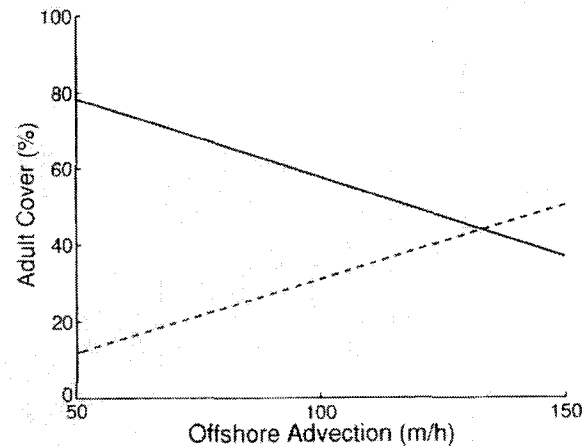

FIG. 4. Adult abundances at equilibrium as functions of offshore advection rate for the competition model. The solid line represents the competitive dominant and the dashed line represents the subordinate.
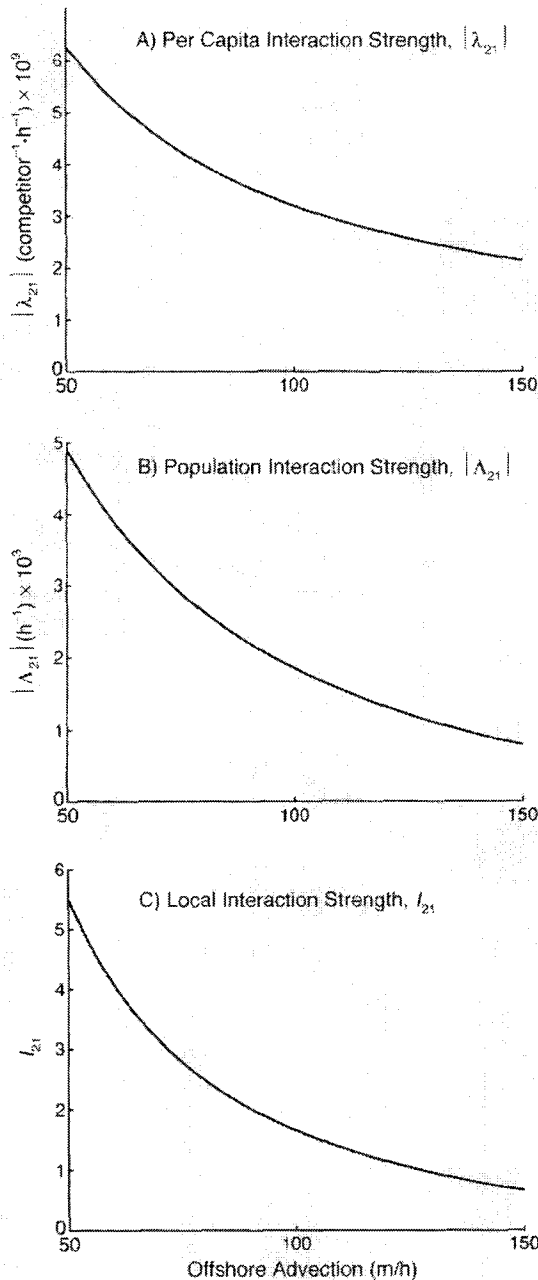
FIG. 5. Magnitudes of competitive interaction strengths of the dominant on the subordinate as functions of the offshore advection rate. Because competition is hierarchical, there is no effect of the subordinate on the dominant. (A) Per capita interaction strength, shown multiplied by a factor of 10^9. (B) Population interaction strength, evaluated at equilibrium and multiplied by 10^3. (C) Local interaction strength, evaluated at equilibrium.

merical analysis indicates that the scaling approximation agrees closely with the full model (Fig. 6), so we refer to the scaling approximation as the "original model" hereafter.

Lotka-Volterra approximation.—Approximating the benthic dynamics with Lotka-Volterra predator–prey equations (see Appendix A) yields

$$r_1 = \frac{(m_1 - \mu_1)p_1}{m_1}$$

$$- \{Ac_2q_2eb_2p_1[Ac_2q_2eb_2(2Ac_1q_1 + 1)$$

$$- 2c_1q_1a_1\mu_2(2Ac_2q_2 + 1)]\}$$

$$\times \{[Ac_2q_2eb_2(2Ac_1q_1 + 1)$$

$$- c_1q_1a_1\mu_2(2Ac_1q_2 + 1)]^2\}^{-1} \qquad (23a)$$

$$r_2 = -\mu_2 \qquad (23b)$$

$$\lambda_{11} = \frac{2c_1q_1a_1m_1(Aeb_2c_2q_2)^2}{[Ac_2q_2eb_2(2Ac_1q_1 + 1) - c_1q_1a_1\mu_2(2Ac_2q_2 + 1)]^2} \qquad (23c)$$

$$\lambda_{22} = 0 \qquad (23d)$$

$$\lambda_{12} = -e \qquad (23e)$$

$$\lambda_{21} = \frac{2Ac_2q_2eb_2}{(2Ac_2q_2 + 1)}. \qquad (23f)$$

As with the competition model, the approximation agrees extremely closely with the original model, even far from the interior equilibrium (Fig. 7).

This Lotka-Volterra model is often written with prey carrying capacity and a predator production coefficient instead of the interaction strengths λ_{11} and λ_{21}. Prey carrying capacity is the prey equilibrium in the absence of the predator:
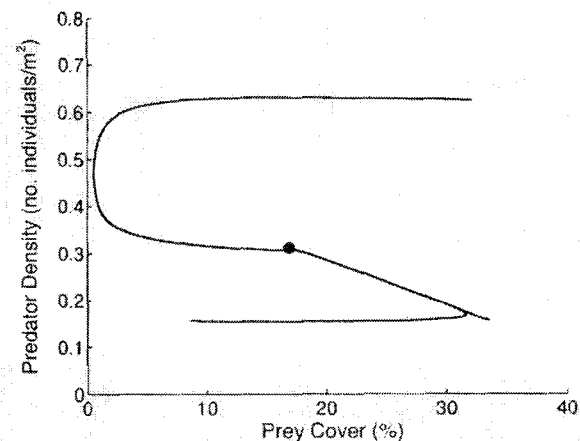

FIG. 6. Comparison of the scaling approximation and the full predator–prey model. The solid lines are trajectories to equilibrium of the full model from three different initial conditions. Trajectories of the scaling approximation from the same three initial conditions are plotted with dashed lines. Dashed lines are not separately visible alongside solid lines, because the trajectories of the two models coincide. The equilibrium is marked with a solid circle. See Fig. 1 for a description of the numerical algorithms. Offshore advection, u, is 100 m/h.
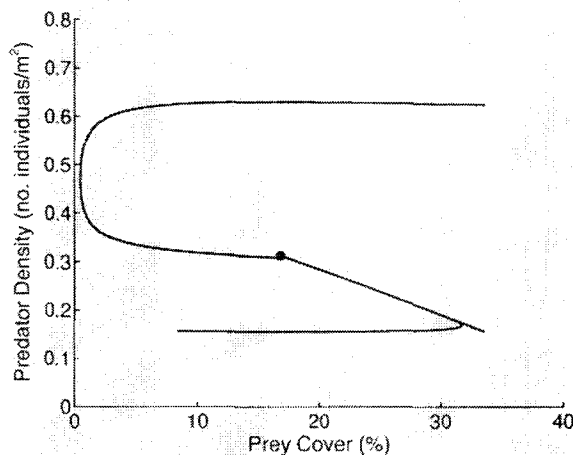
FIG. 7. Comparison of the Lotka-Volterra approximation and the scaling approximation for the predator–prey model. The solid lines are trajectories to equilibrium of the scaling approximation from three different initial conditions. Trajectories of the Lotka-Volterra approximation from the same three initial conditions are plotted with dashed lines. Dashed lines are not separately visible alongside solid lines, because the trajectories of the two models coincide. The equilibrium is marked with a solid circle. The numerical method is described in Fig. 2. Offshore advection, u, is 100 m/h. Note the remarkable similarity between these trajectories and those plotted in Fig. 6.

$$K = -\frac{r_1}{\lambda_{11}}. \tag{24}$$

The predator production coefficient is the number of new adult predators produced per prey consumed:

$$\beta = -\frac{\lambda_{21}}{\lambda_{12}}. \tag{25}$$

Fig. 8 plots the prey intrinsic growth rate, prey carrying capacity, and predator production coefficient as functions of offshore advection. All decrease as upwelling increases.

Adult abundances.—Adult populations equilibrate at

$$\hat{N}_1 = -\frac{r_2}{\lambda_{21}} \tag{26a}$$

$$\hat{N}_2 = \frac{1}{\lambda_{12}}\left(\frac{\lambda_{11}}{\lambda_{21}}r_2 - r_1\right). \tag{26b}$$

Note that the prey equilibrium depends on the predator's life history parameters, but not its own. In particular, when the predator has planktonic larvae, the prey equilibrium depends on the larval transport parameters of the predator, because λ_{21} is a function of q_2 (Eq. 23f). As a result, prey percent cover actually increases as upwelling increases, because strong upwelling inhibits predator recruitment (Fig. 9A). In contrast, predator abundance decreases as upwelling increases (Fig 9B).

Interaction strengths.—The per capita strengths of predator–prey interactions can be obtained directly

from the Lotka-Volterra approximation according to Eq. 1. The per capita effect of predators on prey (Eq. 23e) is independent of upwelling intensity. The per capita effect of prey on predators (Eq. 23f) decreases as upwelling increases (Fig. 10A).

Population interaction strengths (Eq. 2), evaluated at the interior equilibrium, are

$$\Lambda_{12} = -\left(\frac{\lambda_{11}}{\lambda_{21}}r_2 - r_1\right) \tag{27a}$$

$$\Lambda_{21} = -r_2. \tag{27b}$$

In contrast to the per capita effects, the population interaction strength of predators on prey decreases in magnitude as upwelling increases (Fig. 10B), but the population effect of prey on predators is independent of upwelling intensity.

As with the competition model, a submodel simulating predator removal experiments (Appendix B) provides local interaction strength at equilibrium:

$$I_{12} = [Aem_2c_2q_2p_1 - a_1c_1q_1\mu_2(m_1 - \mu_1)(2Ac_2q_2 + 1)]$$
$$\times [a_1c_1q_1\mu_2(m_1 - \mu_1)(2Ac_2q_2 + 1)$$
$$+ Aem_2c_2q_2\mu_1(2Ac_1q_1 + 1)]^{-1}. \tag{28}$$

Fig. 10C illustrates that the local interaction strength of predators on prey decreases as upwelling increases. Again, numerical simulations indicate that this trend holds even when interaction strength is measured before prey abundances have equilibrated (results are not shown).

DISCUSSION

We have developed complex, process-based models coupling benthic adult and pelagic larval dynamics, and have approximated them with simpler, two-equation models for benthic dynamics. These simplified models were approximated with Lotka-Volterra competition and predator–prey equations whose terms are functions of the parameters from the original model. The Lotka-Volterra approximations provide per capita and population interaction strengths. In addition, a submodel that simulates species removal experiments was used to determine local interaction strength. Per capita, population, and local interaction strengths decrease in magnitude or remain constant as upwelling intensity increases (Table 2). We now turn to biological interpretations of these results.

Interaction strength

Per capita interaction strength.—Competition for space occurs in two different ways in the competition model. The first effect is preemptive. Settlement is proportional to free space. Adults consume that space, thereby inhibiting the settlement of larvae adjacent to the coast. This effect is both interspecific and intraspecific. Secondly, larvae of the dominant can settle on subordinate adults. This second interaction is solely
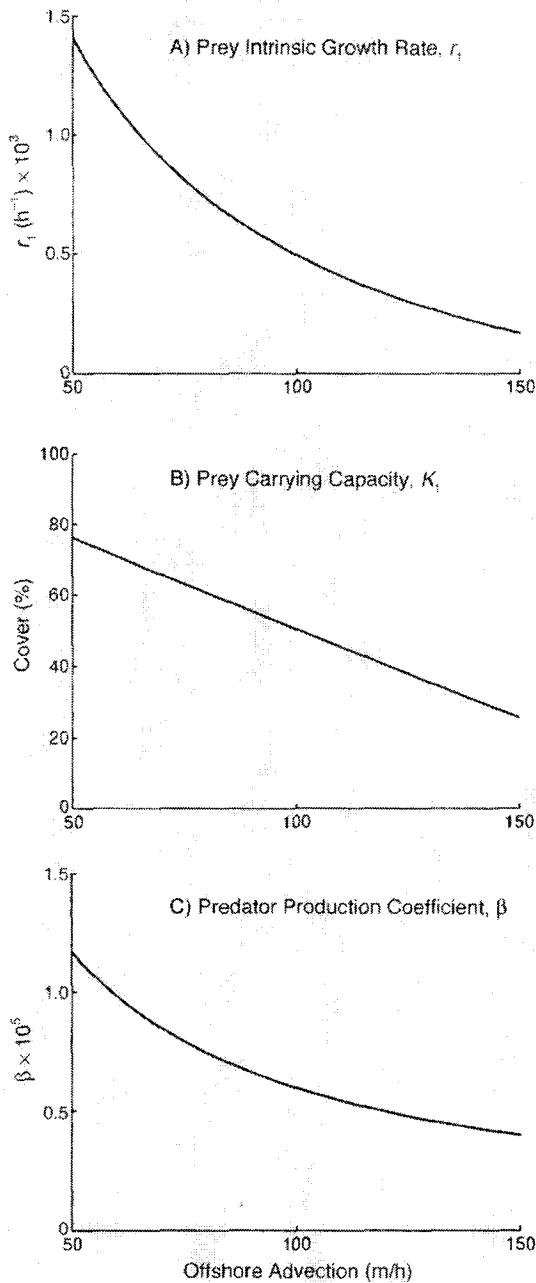
FIG. 8. Sensitivity of Lotka-Volterra parameters (predator–prey model) to offshore advection rate. In panels (A) and (C), y-axis scale numbers have been multiplied by 10^3 and 10^5, respectively.

an adult competitor inhibits the settlement of a smaller proportion of an individual's offspring where upwelling is strong, reducing per capita interaction strength. Note that this interpretation is not specific to offshore advection rate. Rather, it implies that a gradient in any transport process that influences larval supply to the benthic habitat (e.g., proximity of fronts to shore, frequency of relaxation events) should produce a gradient in per capita interaction strength.

Like the per capita competitive effects, the per capita effect of prey on predators (Eq. 23f) decreases as upwelling increases (Fig. 10A). Prey provide the energy needed for predator larval production. Higher proportions of these larvae are swept away from the adult habitat where upwelling is stronger. Thus, the number of predator recruits produced per prey consumed decreases as upwelling increases. As with competitive interaction strength, this interpretation implies that any transport process influencing larval supply should produce a gradient in the per capita effect of prey on predators.

These gradients constrast strikingly with the per capita effect of predators on their prey. This term is independent of upwelling intensity (Eq. 23e). In the two other interactions, the effect of one adult on another's
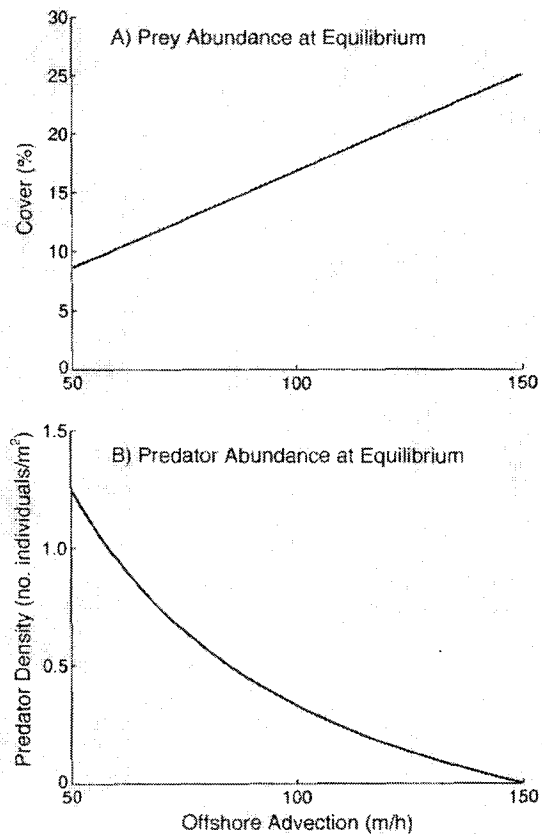

FIG. 9. Adult abundances at equilibrium as functions of offshore advection rate for the predator–prey model.

interspecific, so its effect must be incorporated into the competition coefficient α_{21}. Because α_{21} is relatively insensitive to upwelling (Fig. 3C), we infer that the gradient in per capita interaction strength (Fig. 5A) is driven primarily by the first interaction: inhibition of larval settlement by adults. As upwelling increases, an adult's offspring are advected farther offshore, leaving fewer at the coast to seek settlement sites. Therefore,
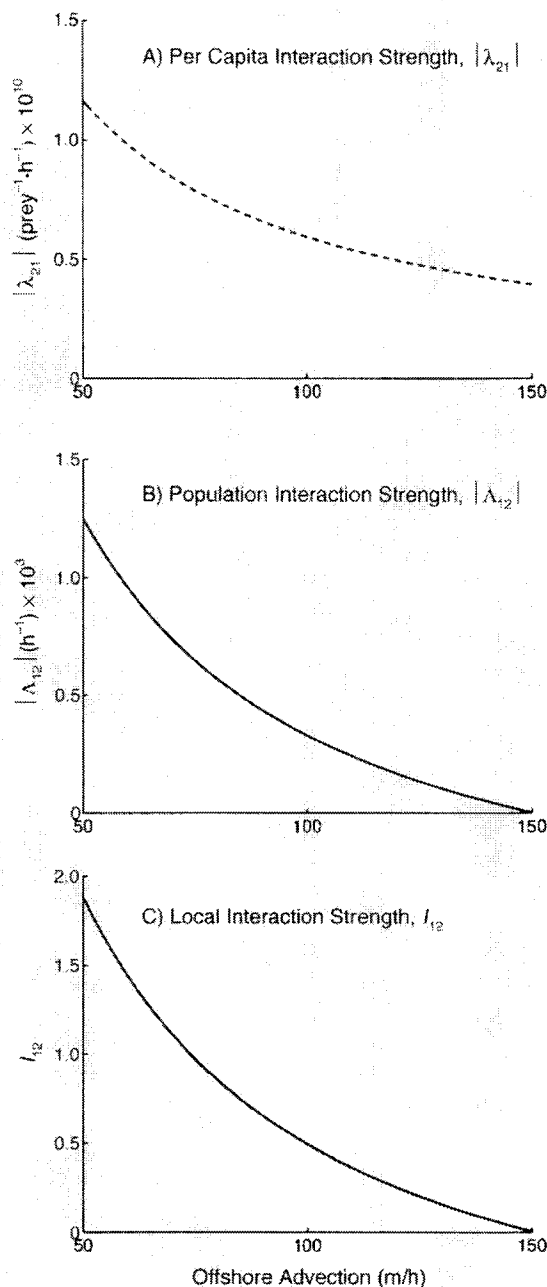
FIG. 10. Magnitudes of predator–prey interaction strengths as functions of the offshore advection rate. (A) Per capita interaction strength of prey on predators, with y-axis scale numbers multiplied by a factor of 10^{10}. The per capita effect of predators on prey is independent of upwelling intensity (Eq. 23e). (B) Population interaction strength of predators on prey, evaluated at equilibrium, shown multiplied by 10^3. The population effect of prey on predators is independent of upwelling intensity (Eq. 27b). (C) Local interaction strength of predators on prey, evaluated at equilibrium.

TABLE 2. Summary of responses of interaction strengths to increasing upwelling.

Metric	Interactions		
	Competitive	Predator–prey	Prey–predator
Per capita	decreases	constant	decreases
Population	decreases	decreases	constant
Local	decreases	decreases	NA†

† Not applicable.

per capita growth rate is mediated through the larval pool. Competition occurs as adults inhibit the settlement of one another's larval offspring. Prey affect predators by influencing the rate of production of predator larvae. The effect of predators on prey, however, is not mediated through the larval pool. Predators do not directly inhibit or facilitate settlement, nor do they influence the prey's per capita rate of larval production. This difference allows the per capita effect of predators on prey to be independent of upwelling intensity.

Population interaction strength.—In the competition model, population interaction strength of the dominant on the subordinate (Eq. 19b) decreases in magnitude as upwelling increases (Fig. 5B). This happens because both the per capita effect and the abundance of dominants decrease as upwelling increases (Figs. 4 and 5A). In the predator–prey model, population interaction strength of the predator on the prey (Eq. 27a) decreases in magnitude as upwelling increases (Fig. 10B). Because the per capita effect is independent of upwelling intensity (Eq. 23e), this gradient is caused by the decreasing predator abundance with increasing upwelling (Fig. 9B). The population interaction strength of prey on predators, however, is independent of upwelling intensity (Eq. 27b). This occurs because the decreasing per capita effect (λ_{21}) is canceled out by increasing prey abundance (λ_{21} in the denominator) (Eqs. 23f and 26a).

Local interaction strength.—In the competition model, recruitment of competitive dominants is lower where upwelling is stronger (Connolly and Roughgarden 1998). This has two consequences. First, the dominant occupies less space in control plots, so more space is available for subordinate settlement. Second, subordinate adults are less likely to be settled on and killed by dominants. These two effects drive the decrease in local interaction strength with increasing upwelling (Fig. 5C). This occurs despite the fact that, in the model, subordinate recruitment is actually higher where upwelling is stronger (Connolly and Roughgarden 1998).

Predator–prey local interaction strength also decreases as upwelling increases (Fig. 10C). Where upwelling is stronger, predator abundance in control plots is lower, so the difference in net prey mortality rate between plots with and without predators is smaller. This produces smaller differences in prey abundance between experimental and control plots where upwelling is stronger.

Other Lotka-Volterra parameters

Alexander and Roughgarden (1996) found that, for the single-species case, intrinsic growth rate and carrying capacity decrease as upwelling increases. The competition and predator–prey models confirm that these qualitative results do not change with the incorporation of a competitor or predator (Figs. 3 and 8). Intrinsic growth rate is the per capita rate of population growth when density-dependent interactions ($\Sigma_j \lambda_{ij} N_j$) are negligible. For a space-limited population, this is the per capita growth rate when benthic free space is abundant, relative to the benthic free space available when the population is at equilibrium. As upwelling increases, the proportion of an adult's larval offspring that are at the coast, seeking settlement sites, decreases; thus, the per capita rate of growth of the benthic population decreases. Carrying capacity is the equilibrium abundance in the absence of the interacting population, and is equal to the ratio of intrinsic growth rate, r_i, to intraspecific (within-species) per capita interaction strength, λ_{ii} (Eqs. 16 and 24). Both intrinsic growth rates (Figs. 3A and 8A) and intraspecific interaction strengths (not shown) decrease in magnitude as upwelling increases; carrying capacity decreases because the former are more sensitive to upwelling than the latter.

Adult abundances

Where stronger upwelling should inhibit recruitment, the subordinate actually equilibrates at a higher percent cover (Fig. 4). This is most easily explained by rewriting Eq. 18b as follows:

$$\hat{N}_2 = K_2 - \alpha_{21} K_1. \qquad (29)$$

Part of the response of subordinate abundance to a gradient in upwelling results from a direct, population-dynamic effect. This is captured by the response of K_2 to changes in upwelling. As Eq. 29 makes clear, there is also a competition-mediated effect. This is captured by the response of $\alpha_{21} K_1$ to changes in upwelling. The competition-mediated effect has two components. Stronger upwelling leads to lower percent cover of the dominant and, therefore, more space on which subordinates can settle. It also leads to lower rates at which dominants settle on and kill subordinates. Because $\alpha_{21} > 1$ and the dominant's carrying capacity is more sensitive to upwelling than the subordinate's (Fig. 3), changes in the competition-mediated effect as upwelling increases (i.e., the gradient in $\alpha_{21} K_1$) outweigh changes in the population-dynamic effect (the gradient in K_2). Consequently, the subordinate benefits from increasing upwelling intensity.

The predator–prey model exhibits similar behavior: prey abundance at equilibrium is lower where upwelling is weaker (Fig 9A). This occurs because prey abundance at equilibrium (Eq. 26a) depends on the predator's life history parameters, but not its own. In par-

ticular, it depends on the larval transport parameters of the predator. This is an example of the top-down control characteristic of Lotka-Volterra predator–prey models, in which increasing the prey's intrinsic growth rate or carrying capacity (in this case, by decreasing upwelling intensity) allows the predator, but not the prey, to increase in abundance (Oksanen et al. 1981).

Agreement with field data

The gradients in abundance predicted by the competition model match data for upper intertidal barnacles in the genera *Balanus* and *Chthamalus* between central California and northern Oregon. The competitively dominant *Balanus* is less abundant in California, where upwelling is strong, than in Oregon, where upwelling is weak. In contrast, the subordinate *Chthamalus* is more abundant in California than in Oregon (Connolly and Roughgarden 1998). The survey during which these data were collected included only the middle and high intertidal zones, above the upper limit of seastars, so those data cannot be used to test the predator–prey model's prediction that prey abundances are higher where upwelling is weaker. Similarly, we cannot confirm that seastars are more abundant in the Pacific Northwest than in central and northern California. The few reports of *Pisaster ochraceus* densities for central and northern California range from $0.5/m^2$ to $4.5/m^2$ (Feder 1956; J. S. Pearse, *unpublished data*) and are within the range of densities reported for Oregon and Washington (Paine 1974, 1976, Menge et al. 1994, Navarrete and Menge 1996). More data are needed to test predicted prey and predator abundance gradients.

Unfortunately, we know of no studies linking regional differences in per capita interaction strength to differences in larval transport processes. Navarrete and Menge (1996) provide a protocol for measuring the per capita interaction strength of predators on prey. By multiplying this term by predator density, population interaction strength can also be estimated. They use this protocol to measure interaction strength on clumps of mussels of fixed densities at different sites, whereas our interaction term corresponds to interaction strength on prey at average densities for a particular upwelling intensity. However, a similar approach could be used to estimate our interaction term. Application of this protocol in different regions of the northeast Pacific (e.g., Oregon and central California) would test two of the model's predictions: (1) between-region differences in per capita interaction strength of predators on prey, if they exist, should be attributable to causes other than larval transport processes; but (2) population interaction strength of predators on prey should tend to be smaller where offshore advection of larvae is stronger (because these regions will sustain lower predator densities). Per capita interaction strengths of prey on predators and of dominant competitors on subordinates depend on larval transport processes, so field estimates of these quantities will require information about the

pelagic larval habitat as well as the benthic adult habitat.

Most field data on interaction strength in intertidal communities come from species removal experiments like those simulated here. Regional differences in the results of seastar removal experiments conducted in the northeast Pacific match those predicted by the model. When seastars are removed from the low intertidal zone, mussel beds expand downward relative to areas where seastars are not removed. This effect decreases in magnitude from northern Washington to central California. In northern Washington, Paine (1974) found a mean rate of expansion of ~0.65 m/yr from 1970 to 1973. In central Oregon, Menge et al. (1994) found mean rates of expansion of ~0.5 m/yr at one site and 0.25 m/yr at another from 1990 to 1993. In central California, J. S. Pearse (*unpublished data*) found a smaller effect, expansion at a mean rate of <0.1 m/yr from 1979 to 1985. The effect of predator exclusion on barnacles shows the same trend. In central California, a predator exclusion experiment found that barnacle cover increased by ~30% (from 40% to 70% cover) over 9 mo (T. M. Farrell, *unpublished data*). This contrasts starkly with Dayton's (1971) classic experiments in northern Washington, in which barnacle cover increased from nearly 0% to nearly 100% in the first 9 mo. Although these studies were not identical in design, were conducted at different times, and did not quanitify the relative contributions of recruitment and individual growth to the results, the trends in both mussel and barnacle experiments match the model's prediction: smaller effects in the region of stronger upwelling.

Robustness of model predictions

To make the interpretation of results as unambiguous as possible, we used simple functions to characterize competition and predation and considered two well-mixed, interacting populations isolated from the rest of the community. The simplifying assumptions made in the process fall into two broad classes. The first class pertains to the form of the per capita interactions in the model. The second class mediates the effects of these interactions at the population level. The models presented in this paper provide a framework for thoroughly exploring these assumptions, because they can be modified, and reanalyzed, with the new results compared to those reported here. An extensive treatment of such modifications is beyond the scope of this paper. However, a preliminary investigation of both classes of assumptions suggests that the central result of this paper is robust: interaction strengths decrease or remain constant as upwelling increases. We now briefly summarize this investigation.

Functional form of per capita interactions.—Two assumptions about the form of the per capita interactions that may be relaxed in the northeast Pacific rocky intertidal zone are density-independent adult mortality

and linearly increasing predation rate with prey density. The assumption that the adult mortality rate is independent of density is violated when free space is scarce (Gaines and Roughgarden 1985). To investigate the sensitivity of our results to this assumption, we modified the competition model to include a simple representation of density dependence, linearly increasing mortality with adult density. This increases per capita interaction strengths because individuals not only inhibit the settlement of larvae, but also directly increase the mortality rates of other adults. However, per capita, population, and local interaction strengths still decrease in magnitude as upwelling increases (results are not shown). For the predator–prey interaction, we cannot confirm the assumption that the predation rate increases linearly with prey density. Therefore, to explore the sensitivity of our results to predator satiation, we used

$$\frac{eN_i(t)}{D + N_i(t)} \tag{30}$$

to characterize predation rate instead of the $-eN_i(t)$ of Eqs. 8–9 (Holling 1965). Here, e is the maximum predation rate per predator, and D is a constant set so that e/D is the slope of the functional response curve at $N_i = 0$; i.e., e/D is the predation rate per predator at very low prey density. With this modification, the per capita effect of predators on prey decreases, rather than remaining constant, as upwelling increases, while all other trends are unchanged in direction (results are not shown).

Population-level processes.—The models presented here examine two well-mixed populations isolated from the rest of the community. As in the classical Lotka-Volterra predator–prey model, these models allow one population to strongly control the abundance of another along an environmental gradient (Oksanen et al. 1981). Neither the competitive subordinate nor the prey is able to benefit from weak upwelling intensity, because the direct, population-dynamic benefits are outweighted by increased abundance and recruitment of the dominant or predator. Previous work has shown that realistic modifications to two population models, such as additional species interactions, prey refuges, or nonequilibrium dynamics, can mediate this strong interspecific control of population abundances (see reviews in Pimm 1991, DeAngelis 1992, Polis and Winemiller 1996). Although the explicit incorporation of additional populations, refuges, and spatial and temporal stochasticity is beyond the scope of this paper, we can consider the sensitivity of our results to predicted abundance gradients by evaluating interaction strengths at prey and subordinate abundances other than their equilibrium values. As an extreme case, consider interaction strengths evaluated at prey and subordinate carrying capacities. In contrast to equilibrium abundances, these quantities decrease as upwelling increases. Thus, any gradient in interaction strength that is sensitive to strong top-down or competitive control

of abundance should change direction when evaluated at carrying capacity. Nevertheless, we found that this modification does not change the direction of the gradients in per capita interaction strengths or local interaction strengths. Similarly, neither the population interaction strengths in the competition model nor the population interaction strength of predators on prey are changed in direction. However, the population interaction strength of prey on predators does change: when evaluated at prey carrying capacity, it decreases, rather than remaining constant, as upwelling increases (results are not shown).

This preliminary investigation suggests that the results that are likely to be sensitive to relaxation of model assumptions are those that are independent of upwelling in the original analysis: the per capita effect of predators on prey and the population effect of prey on predators. Interaction strengths that decrease as upwelling increases under the original analysis do not change direction. Note that this reinforces the overall tendency for interaction strengths to decrease as upwelling increases. Although we cannot guarantee that this tendency for species interactions to become weaker as upwelling increases will hold under any conceivable set of assumptions, this preliminary investigation indicates that it is not an artifact of the particular set of assumptions adopted for the models analyzed in this paper.

Conclusions

These results support the hypothesis that geographical gradients in larval transport processes produce gradients in interaction strength. These gradients can be driven by changes in per capita effects, changes in abundance, or both. The decreasing competitive interaction strength with increasing upwelling is driven by both decreasing per capita effects and decreasing abundance of the dominant. The decreasing population interaction strength of predators on prey with increasing upwelling is driven entirely by decreasing predator abundance. Conversely, the decreasing per capita effect of prey on predators with increasing upwelling is canceled out at the population level by increasing prey abundance.

A striking result of this study is the concordance between the responses of local and population interaction strengths to a gradient in upwelling intensity (Table 2). This indicates that a latitudinal gradient in upwelling may be responsible for geographical differences in the results of species removal experiments in the northeast Pacific (Roughgarden et al. 1988), and that these differences reflect population-level differences in the intensity of competition and predation. The qualitative agreement between local and population interaction strengths is encouraging, because much of our information about intertidal communities comes from local experiments. However, we caution that local interaction strengths are not identical to population in-

teraction strengths, so the positive correlation between local and population interaction strength found here may not hold for all environmental gradients.

Considerable empirical work has been done to construct and analyze interaction webs for rocky intertidal communities (e.g., Paine 1980, Menge 1995, Wootton 1997). The assembly of these webs has been based on experimental manipulations on the scale of meters. For most benthic marine animals, communities at this scale are almost entirely open, in that virtually none of the recruits to experimental plots will have been produced by adults in those same plots. In contrast, most theory for interaction webs is formulated for closed systems (see reviews in Pimm 1982, 1991, DeAngelis 1992, Polis and Winemiller 1996). To compare community structure patterns across marine, terrestrial, and aquatic systems, we need a theoretical framework for marine communities that allows us to construct population-level webs for benthic marine communities. By demonstrating that per capita and population interaction strengths can be expressed in terms of measurable life history parameters, this paper provides a step in that direction.

LITERATURE CITED

Alexander, S. E., and J. Roughgarden. 1996. Larval transport and population dynamics of intertidal barnacles: a coupled benthic/oceanic model. Ecological Monographs 66:259–275.

Booth, D. J., and D. M. Brosnan. 1995. The role of recruitment dynamics in rocky shore and coral reef fish communities. Advances in Ecological Research 26:309–385.

Brown, S. K., and J. Roughgarden. 1985. Growth, morphology, and laboratory culture of larvae of *Balanus glandula* (Cirripedia: Thoracica). Journal of Crustacean Biology 5:574–590.

Connell, J. H. 1961. The influence of interspecific competition and other factors on the distribution of the barnacle *Chthamalus stellatus*. Ecology 42:710–723.

———. 1985. The consequences of variation in initial settlement vs. post-settlement mortality in rocky intertidal communities. Journal of Experimental Marine Biology and Ecology 93:11–45.

Connolly, S. R., and J. Roughgarden. 1998. A latitudinal gradient in intertidal community structure: evidence for an oceanographically-based synthesis of marine community theory. American Naturalist 151:311–326.

Dayton, P. K. 1971. Competition, disturbance, and community organization: the provision and subsequent utilization of space in a rocky intertidal community. Ecological Monographs 41:351–389.

DeAngelis, D. A. 1992. Dynamics of nutrient cycling and food webs. Chapman and Hall, London, UK.

Denny. M. W., and M. F. Shibata. 1989. Consequences of surf-zone turbulence for settlement and external fertilization. American Naturalist 134:859–889.

Dial. R. J., and J. Roughgarden. 1998. Theory of marine communities: the intermediate disturbance hypothesis. Ecology 79:1412–1424.

Ebert, T. A. 1996. The consequences of broadcasting, brooding, and asexual reproduction in echinoderm metapopulations. Oceanologica Acta 19:217–226.

Ebert, T. A., and M. P. Russell. 1988. Latitudinal variation in size structure of the west coast purple sea urchin: a correlation with headlands. Limnology and Oceanography 33:286–294.

Fairweather, P. G. 1988. Consequences of supply-side ecology: manipulating the recruitment of intertidal barnacles affects the intensity of predation upon them. Biological Bulletin 175:349–354.

Farrell, T. M. 1989. Succession in a rocky intertidal community: the importance of disturbance size and position within a disturbed patch. Journal of Experimental Marine Biology and Ecology 128:57–73.

———. 1991. Models and mechanisms of succession: an example from a rocky intertidal community. Ecological Monographs 61:95–113.

Farrell, T. M., D. Bracher, and J. Roughgarden. 1991. Cross-shelf transport causes recruitment to intertidal populations in central California. Limnology and Oceanography 36:279–288.

Feder, H. M. 1956. Natural history studies on the starfish Pisaster ochraceus (Brandt, 1835) in the Monterey Bay area. Dissertation. Stanford University. Stanford, California, USA.

Gaines, S. D., and M. D. Bertness. 1992. Dispersal of juveniles and variable recruitment in sessile marine species. Nature 360:579–580.

Gaines, S. D., S. Brown, and J. Roughgarden. 1985. Spatial variation in larval concentrations as a cause of spatial variation in settlement for the barnacle, Balanus glandula. Oecologia 67:267–272.

Gaines, S. D., and K. D. Lafferty. 1995. Modeling the dynamics of marine species: the importance of incorporating larval dispersal. Pages 389–412 in L. McEdward, editor. Ecology of marine invertebrate larvae. CRC Press. Boca Raton, Florida, USA.

Gaines, S. D., and J. Roughgarden. 1985. Larval settlement rate: a leading determinant of structure in an ecological community of the marine intertidal zone. Proceedings of the National Academy of Sciences, (USA) 82:3707–3711.

Grantham, B. A. 1997. Coastal upwelling, larval recruitment, and the dynamics of upper intertidal barnacle communities. Dissertation. Stanford University. Stanford, California, USA.

Harrold, C. 1981. Feeding ecology of the asteroid Pisaster giganteus in a kelp forest system: prey selection, predator-prey interactions, and energetics. Dissertation. University of California, Santa Cruz, California, USA.

Hastings, A. 1980. Disturbance, coexistence, history, and competition for space. Theoretical Population Biology 18:363–373.

Hines, A. H. 1976. Comparative reproductive ecology of three species of intertidal barnacles. Dissertation. University of California, Berkeley, California, USA.

Hirsch, C. 1988. Numerical computation of internal and external flows. John Wiley and Sons, New York, New York, USA.

Holling, C. S. 1965. The functional response of predators to prey density and its role in mimicry and population regulation. Memoirs of the Entomological Society of Canada 45:3–60.

Holmes, E. E., M. A. Lewis, J. E. Banks, and R. R. Ueit.

———. 1994. Partial differential equations in ecology: spatial interactions and population dynamics. Ecology 75:17–29.

Huyer, A. 1983. Coastal upwelling in the California Current system. Progress in Oceanography 12:259–284.

Iwasa, Y., and J. Roughgarden. 1986. Interspecific competition among metapopulations with space-limited subpopulations. Theoretical Population Biology 30:194–214.

Mann, K. H., and J. R. N. Lazier. 1996. Dynamics of marine ecosystems: biological–physical interactions in the oceans. Second edition. Blackwell, Boston, Massachusetts, USA.

MATLAB. 1994. MATLAB version 4.2c. The Math Works, Natick, Massachusetts, USA.

Menge, B. A. 1975. Brood or broadcast? The adaptive significance of different reproductive strategies in the two intertidal sea stars Leptasterias hexactis and Pisaster ochraceus. Marine Biology 31:87–100.

———. 1991. Relative importance of recruitment and other causes of variation in rocky intertidal community structure. Journal of Experimental Marine Biology and Ecology 146:69–100.

———. 1995. Indirect effects in marine rocky intertidal interaction webs: patterns and importance. Ecological Monographs 65:21–74.

Menge, B. A., E. L. Berlow, C. A. Blanchette, S. A. Navarrete, and S. B. Yamada. 1994. The keystone species concept: variation in interaction strength in a rocky intertidal habitat. Ecological Monographs 64:249–286.

Menge, B. A., and T. M. Farrell. 1989. Community structure and interaction webs in shallow marine hard-bottom communities: test of an environmental stress model. Advances in Ecological Research 19:189–262.

Menge, B. A., and J. P. Sutherland. 1987. Community regulation: variation in disturbance, competition, and predation in relation to environmental stress and recruitment. American Naturalist 130:730–757.

Miller, K. M. 1992. The biology of barnacles. Dissertation. Stanford University. Stanford, California, USA.

Miller, K. M., S. M. Blower, D. Hedgecock, and J. Roughgarden. 1989. Comparison of larval and adult stages of Chthamalus dalli and Chthamalus fissus (Cirripedia: Thoracica). Journal of Crustacean Biology 9:242–256.

Navarrete, S. A., and B. A. Menge. 1996. Keystone predation and interaction strength: interactive effects of predators on their main prey. Ecological Monographs 66:409–429.

Newman, W. M., and D. P. Abbott. 1980. Cirripedia: the barnacles. Pages 504–535 in R. H. Morris, D. P. Abbott, and E. C. Haderlie, editors. Intertidal invertebrates of California. Stanford University Press. Stanford, California, USA.

Nimitz, Sister M. A. 1971. Histochemical study of gut nutrient reserves in relation to reproduction and nutrition in the sea stars. Pisaster ochraceus and Patiria miniata. Biological Bulletin 140:461–481.

Oksanen, L., S. D. Fretwell, J. Arruda, and P. Niemela. 1981. Exploitation ecosystems in gradients of primary productivity. American Naturalist 118:240–261.

Okubo, A. 1971. Oceanic diffusion diagrams. Deep Sea Research 18:789–802.

———. 1980. Diffusion and ecological problems: mathematical models. Springer-Verlag. Berlin, Germany.

Paine, R. T. 1966. Food web complexity and species diversity. American Naturalist 100:65–75.

———. 1974. Intertidal community structure. Experimental studies on the relationship between a dominant competitor and its principal predator. Oecologia 15:93–120.

———. 1976. Size-limited predation: an observational and experimental approach with the Mytilus–Pisaster interaction. Ecology 57:858–873.

———. 1980. Food webs: linkage, interaction strength and

community structure. Journal of Animal Ecology **49**:667–685.

———. 1992. Food-web analysis through field measurements of per capita interaction strength. Nature **355**:73–75.

———. 1994. Marine rocky shores and community ecology: an experimentalist's perspective. Ecology Institute, Oldendorf/Luhe, Germany.

Parrish, R. H., C. S. Nelson, and A. Bakun. 1981. Transport mechanisms and the reproductive success of fishes in the California Current. Biological Oceanography **1**:175–203.

Patankar, S. V. 1980. Numerical heat transfer and fluid flow. McGraw-Hill, New York, New York, USA.

Petersen, J. H. 1984. Larval settlement behavior in competing species: *Mytilus californianus* Conrad and *M. edulis* L. Journal of Experimental Marine Biology and Ecology **82**:147–159.

Pimm, S. L. 1982. Food webs. Chapman and Hall, London, UK.

———. 1991. The balance of nature? University of Chicago Press, Chicago, Illinois, USA.

Piñeda, J. 1991. Predictable upwelling and the shoreward transport of planktonic larvae by internal tidal bores. Science **253**:548–551.

Polis, G. A., and K. O. Winemiller, editors. 1996. Food webs: integration of patterns and dynamics. Chapman and Hall, New York, New York, USA.

Pond, S., and G. L. Pickard. 1995. Introductory dynamical oceanography. Second edition. Butterworth-Heinemann, Oxford, UK.

Possingham, H. P., and J. Roughgarden. 1990. Spatial population dynamics of a marine organism with a complex life cycle. Ecology **71**:973–985.

Possingham, H. P., S. Tuljapurkar, J. Roughgarden, and M. Wilks. 1994. Population cycling in space-limited organisms subject to density-dependent predation. American Naturalist **143**:563–582.

Pyefinch, K. A. 1948. Methods of the identification of the larvae of *Balanus balanoides* (L.), *B. crenatus* Brug, and *Verruca stroemia* O. F. Muller. Journal of the Marine Biological Association of the United Kingdom **28**:353–369.

Robles, C. D. 1997. Changing recruitment in constant species assemblages: implications for predation theory in intertidal communities. Ecology **78**:1400–1414.

Roughgarden, J. 1986. A comparison of food-limited and space-limited animal competition communities. Pages 492–516 *in* J. Diamond and T. Case, editors. Community Ecology. Harper and Row, New York, New York, USA.

Roughgarden, J., S. D. Gaines, and H. Possingham. 1988. Recruitment dynamics in complex life cycles. Science **241**: 1460–1466.

Roughgarden, J., J. T. Pennington, and S. Alexander. 1994. Dynamics of the rocky intertidal zone with remarks on generalization in ecology. Philosophical Transactions of the Royal Society of London Series B **343**:79–85.

Roughgarden, J., J. T. Pennington, D. Stoner, S. Alexander, and K. Miller. 1991. Collisions of upwelling fronts with the intertidal zone: the cause of recruitment pulses in barnacle populations of central California. Acta Oecologia **12**: 35–51.

Satchell, E. R., and T. M. Farrell. 1993. Effects of settlement density on spatial arrangement in four intertidal barnacles. Marine Biology **116**:241–245.

Seed, R. 1976. Ecology. Pages 13–65 *in* B. L. Bayne, editor. Marine mussels: their ecology and physiology. Cambridge University Press, London, UK.

Sewell, M. A., and D. R. Levitan. 1992. Fertilization success during a natural spawning of the dendrochirote sea cucumber *Cucumaria miniata*. Bulletin of Marine Science **51**: 161–166.

Shanks, A. L. 1983. Surface slicks associated with tidally-forced internal waves may transport pelagic larvae of benthic invertebrates and fishes shoreward. Marine Ecology Progress Series **13**:311–315.

Strathmann, M. F. 1987. Reproduction and development of marine invertebrates of the northern Pacific coast. University of Washington Press, Seattle, Washington, USA.

Strathmann, R. R. 1978. Length of pelagic period in echinoderms with feeding larvae from the northeast Pacific. Journal of Experimental Marine Biology and Ecology **34**: 23–27.

———. 1996. Are planktonic larvae of benthic marine invertebrates too scarce to compete within species? Oceanologica Acta **19**:399–407.

Strathmann, R. R., and K. Vedder. 1978. Size and organic content of eggs of echinoderms and other invertebrates as related to developmental strategies and egg eating. Marine Biology **39**:305–309.

Tilman, D. 1994. Competition and biodiversity in spatially structured habitats. Ecology **75**:2–16.

Turner, R. L., and J. M. Lawrence. 1979. Volume and composition of echinoderm eggs: implications for the use of egg size in life history models. Pages 25–40 *in* S. E. Stancyk, editor. Reproductive ecology of marine invertebrates. University of South Carolina Press, Columbia, South Carolina, USA.

Underwood, A. J., and E. J. Denley. 1984. Paradigms, explanations, and generalizations in models for the structure of intertidal communities on rocky shores. Pages 151–180 *in* D. R. Strong, D. Simberloff, L. G. Abele, and A. B. Thistle, editors. Ecological communities: conceptual issues and the evidence. Princeton University Press, Princeton, New Jersey, USA.

Underwood, A. J., E. J. Denley, and M. J. Moran. 1983. Experimental analyses of the structure and dynamics of mid-shore rocky intertidal communities in New South Wales. Oecologia **56**:202–219.

U.S. GLOBEC. 1994. Eastern Boundary Current Program: a science plan for the California Current. U.S. Global Ocean Ecosystems Dynamics, Report No. 11. U.S. GLOBEC Scientific Steering Coordinating Office, Berkeley, California, USA.

Wing, S. R., L. W. Botsford, J. L. Largier, and L. E. Morgan. 1995. Spatial structure of relaxation events and crab settlement in the northern California upwelling system. Marine Ecology Progress Series **128**:199–211.

Wootton, J. T. 1997. Estimates and tests of per capita interaction strength: diet, abundance, and impact of intertidally foraging birds. Ecological Monographs **67**:45–64.

APPENDIX A

LOTKA-VOLTERRA APPROXIMATION

Competition model

The Lotka-Volterra equations for two species can be written in the form

$$\frac{dN_1}{dt} = [r_1 + \lambda_{11}N_1 + \lambda_{12}N_2]N_1 \tag{A.1a}$$

$$\frac{dN_2}{dt} = [r_2 + \lambda_{21}N_1 + \lambda_{22}N_2]N_2. \tag{A.1b}$$

We wish to obtain a model of this form that approximates the model of Eq. 13. Therefore, throughout this appendix, dN_1/dt and dN_2/dt refer to Eqs. 13a and 13b, respectively. To insure that the approximation has the same interior equilibrium as the original model, we evaluate the approximation at this equilibrium. Thus, the interior equilibrium of the original model,

$$\hat{N}_1 = \frac{p_1}{2a_2c_1q_1(m_1 - \mu_1)} \tag{A.2a}$$

$$\hat{N}_2 = [c_1q_1(m_1 - \mu_1)(a_2p_1 + a_1\mu_2)$$

$$+ c_2q_2\mu_1(a_2p_1 - a_1(m_2 - \mu_2))]$$

$$\div [2a_2c_1q_1c_2q_2(m_1 - \mu_1)(a_2p_1 - a_1(m_2 - \mu_2))] \tag{A.2b}$$

(Connolly and Roughgarden 1998), will be equal to the interior equilibrium of the Lotka-Volterra model (Eq. 18).

First, we differentiate Eqs. 13a and A.1a with respect to N_2:

$$\frac{\partial}{\partial N_2}\left(\frac{dN_1}{dt}\right) = \lambda_{12}N_1. \tag{A.3}$$

Solving this expression for λ_{12} and evaluating, we get Eq. 14e. Next, differentiating Eqs. 13a and A.1a with respect to N_1, we obtain

$$\frac{\partial}{\partial N_1}\left(\frac{dN_1}{dt}\right) = r_1 + 2\lambda_{11}N_1. \tag{A.4}$$

Evaluating both sides at their respective interior equilibria, λ_{11} drops out and we can obtain r_1 (Eq. 14a). We then set Eq. A.1a equal to zero and solve for λ_{11}:

$$\lambda_{11} = -\frac{r_1}{\hat{N}_1}. \tag{A.5}$$

Evaluating at the interior equilibrium, we get Eq. 14c. Differentiating Eqs. 13b and A.1b with respect to N_1, we get

$$\frac{\partial}{\partial N_1}\left(\frac{dN_2}{dt}\right) = \lambda_{21}N_2. \tag{A.6}$$

Solving this expression for λ_{21} and evaluating at the interior equilibrium, we get Eq. 14f. Now, differentiating Eqs. 13b and A.1b with respect to N_2, we obtain

$$\frac{\partial}{\partial N_2}\left(\frac{dN_2}{dt}\right) = r_2 + \lambda_{21}N_1 + 2\lambda_{22}N_2. \tag{A.7}$$

Evaluating both sides of this expression at their respective interior equilibria, λ_{22} vanishes and we can solve for r_2 (Eq. 14b). We can then set Eq. A.1b equal to zero, solve for λ_{22} and evaluate at the interior equilibrium of the original model, yielding Eq. 14d.

Note that r_1 and λ_{11} correspond to r and λ for a single-species model, because competition is hierarchical. In addition, as the dominant approaches its extinction threshold ($p_2 \to 0$), r_2 and λ_{22} also approach the single-species expressions.

Predator-prey model

Again, we write the Lotka-Volterra equations in the form of Eq. A.1, where dN_1/dt and dN_2/dt refer to the appropriate equations from the scaling approximation (Eq. 21). The interior equilibrium of the original model is

$$\hat{N}_1 = \frac{\mu_2(2Ac_2q_2 + 1)}{2Ac_2q_2em_2} \tag{A.8a}$$

$$\hat{N}_2 = \{c_1q_1(m_1 - \mu_1)[2Ac_2q_2(Aem_2 - a_1\mu_2) - a_1\mu_2]$$

$$- Ac_2q_2em_2\mu_1\}$$

$$\times \{e(c_1q_1[2Ac_2q_2(Aem_2 - a_1\mu_2) - a_1\mu_2]$$

$$+ Ac_2q_2em_2)\}^{-1}. \tag{A.8b}$$

Because there is no effect of predators on one another, $\lambda_{22} = 0$, and the Lotka-Volterra equilibrium is given by Eq. 26.

First, we differentiate Eqs. 21a and A.1a with respect to N_2 to obtain

$$\frac{\partial}{\partial N_2}\left(\frac{dN_1}{dt}\right) = \lambda_{12}N_1. \tag{A.9}$$

Solving this expression for λ_{12}, we get Eq. 23e. Similarly, from

$$\frac{\partial}{\partial N_1}\left(\frac{dN_2}{dt}\right) = \lambda_{21}N_2 \tag{A.10}$$

we can solve for λ_{21} (Eq. 23f). Differentiating Eqs. 21b and A.1b with respect to N_2, we obtain

$$\frac{\partial}{\partial N_2}\left(\frac{dN_2}{dt}\right) = r_2 + \lambda_{21}N_1. \tag{A.11}$$

Solving for r_2 and evaluating at the interior equilibrium of the original model, we get Eq. 23b. Next, we differentiate Eqs. 21a and A.1a with respect to N_1:

$$\frac{\partial}{\partial N_1}\left(\frac{dN_1}{dt}\right) = r_1 + 2\lambda_{11}N_1 + \lambda_{12}N_2. \tag{A.12}$$

Evaluating each side at its respective interior equilibrium, the unknown r_1 drops out, and we can solve for λ_{11} (Eq. 23c). Finally, we set Eq. A.1a equal to zero, solve for r_1, and evaluate at the interior equilibrium of the original model, yielding Eq. 23a.

APPENDIX B

DERIVATION OF LOCAL INTERACTION STRENGTH

Competition model

The submodel used to derive local interaction strength is based on two observations about species removal experiments. First, abundances in experimentally manipulated plots are small relative to the sizes of the regional breeding populations whose larvae recruit to the plots. Second, the dominant and subordinate coexist in the system as a whole. If these assumptions hold, larval abundances adjacent to both experimental and control plots are simply $L_1(0, N_1)$ and $L_2(0, N_1, N_2)$ (Eq. 11). Here, we assume that the regional system is at equi-

librium and evaluate larval abundances accordingly. Population dynamics in the control (dominant present) plot follow

$$\frac{dN_1^C(t)}{dt} = c_1\hat{L}_1(0, \hat{N}_1)[F^C(t) + a_2 N_2^C(t)] - \mu_1 N_1^C(t) \quad \text{(B.1a)}$$

$$\frac{dN_2^C}{dt} = c_2\hat{L}_2(0, \hat{N}_1, \hat{N}_2)F^C(t) - \mu_2 N_2^C(t)$$

$$- c_1\hat{L}_1(0, \hat{N}_1)a_2 N_2^C(t) \quad \text{(B.1b)}$$

$$F^C(t) = A - a_1 N_1^C(t) - a_2 N_2^C(t), \quad \text{(B.1c)}$$

and subordinate dynamics in the experimental (dominant removed) plot follow

$$\frac{dN_2^E}{dt} = c_2 L_2(0, \hat{N}_1, \hat{N}_2)F^E(t) - \mu_2 N_2^E(t) \quad \text{(B.2a)}$$

$$F^E(t) = A - a_2 N_2^E(t). \quad \text{(B.2b)}$$

The superscript C refers to the control plot, and E refers to the experimental plot. Local interaction strength can be measured by comparing abundances in both plots according to Eq. 3. At equilibrium, subordinate abundance in the control plot is given by Eq. A.2b, and subordinate abundance in the experimental plot is

$$\hat{N}_2^E = \frac{A}{a_2}([c_1 q_1(m_1 - \mu_1)(a_2 p_1 + a_1\mu_2)$$

$$+ c_2 q_2\mu_1(a_2 p_1 - a_1(m_2 - \mu_2))]$$

$$\times \{c_1 q_1 a_2 p_1(m_1 - \mu_1)$$

$$+ c_2 q_2\mu_1[a_2 p_1 - a_1(m_2 - \mu_2)]\}^{-1}). \quad \text{(B.3)}$$

Local interaction strength evaluates to Eq. 20.

Predator–prey model

Following the procedure just outlined, prey dynamics in predator removal experiments can be simulated. Population dynamics in the control (predator present) plot follow

$$\frac{dN_1^C(t)}{dt} = c_1\hat{L}_1(0, \hat{N}_1)F^C(t) - \mu_1 N_1(t)$$

$$- eN_1^C(t)N_2^C(t) \quad \text{(B.4a)}$$

$$\frac{dN_2^C(t)}{dt} = c_2 A\hat{L}_2(0, \hat{N}_1, \hat{N}_2) - \mu_2 N_2^C(t) \quad \text{(B.4b)}$$

$$F^C(t) = A - a_1 N_1^C(t). \quad \text{(B.4c)}$$

Prey dynamics in experimental (predator-removed) plots follow

$$\frac{dN_1^E(t)}{dt} = c_1\hat{L}_1(0, \hat{N}_1)F^E(t) - \mu_1 N_1^E(t) \quad \text{(B.5a)}$$

$$F(t) = A - a_1 N_1^E(t). \quad \text{(B.5b)}$$

At equilibrium, prey abundance in the control plot is given by Eq. A.8a, and prey abundance in the experimental plot is

$$\hat{N}_1^E = [Ac_1 q_1 m_1\mu_2(2Ac_2 q_2 + 1)]$$

$$\times [Aem_2\mu_1 c_2 q_2(2Ac_1 q_1 + 1)$$

$$- c_1 q_1 a_1\mu_2(m_1 - \mu_1)(2Ac_2 q_2 + 1)]^{-1}. \quad \text{(B.6)}$$

Local interaction strength evaluates to Eq. 28.

SUPPLEMENTARY MATERIAL

Scripts for the simulations reported in this paper are available in ESA's Electronic Data Archive: *Ecological Archives* M069-004.